Zinc 2-((2-(Benzoimidazol-2-yl)quinolin-8-ylimino)methyl)phenolates: Synthesis, characterization and photoluminescence behavior

Longlong Li, Xian Zhang, Wenjuan Zhang, Wen Li, Wen-Hua Sun, Carl Redshaw

Abstract

A series of 2-(2-(*1H*-benzoimidazol-2-yl)quinolin-8-yliminomethyl)phenol derivatives and their zinc complexes (**C1 – C5**) were synthesized and fully characterized. The molecular structure of the representative complex **C2** was determined by single crystal X-ray diffraction, which revealed that the zinc was five-coordinated with the tetra-dentate ligand and a methanol bound to the metal afford a distorted square-pyramidal geometry. The UV-Vis absorption and fluorescence spectra of the organic compounds and their zinc complexes were measured and investigated in various solvents such as methanol, THF, dichloromethane, and toluene; significant influences by solvents were observed on their luminescent properties; red-shifts for the zinc complexes were clearly observed in comparisons to the free organic compounds.

Keywords: 2-(2-(*1H*-Benzoimidazol-2-yl)quinolin-8-yliminomethyl)phenol; tetra-dentate ligand; zinc complexes; fluorescence; UV-absorption spectra

Introduction

Luminescent materials of both organic compounds and metal complexes continue to attract interest as organic light emitting diodes (OLEDs), photo-sensitizers, sensitive DNA probes for signaling, and molecular switches [1-6]. Within these compounds, the use of zinc complexes has has become popular over the past decades due to their enhanced thermal stability and fluorescent properties which are enhanced *versus* the 'free ligands' [16-20]. Zinc itself has been recognized as the second abundant metal in human body [7], and is involved in various biological processes including DNA synthesis, microtubule polymerization, gene expression, apoptosis, immune system function, as well enzyme activity [8-11]; meanwhile unbalances of the zinc ion can cause neurological disorders to result: amyotrophic lateral sclerosis and diseases such as Alzheimers, Parkinson, and epilepsy [12-15]. In chemical terms, the multi-dentate zinc complexes have been extensively explored for their fluorescent properties [21-27] by employing easily available Schiff-base ligands, moreover, the versatility of their structures are also attractive [28-32]. We have also investigated several series of multi-dentate zinc complexes [25-27, 33, 34], and observed good photoluminescence behavior for zinc complexes bearing 2-(*1H*-benzoimidazol-2-yl)-substituted quinolin-8-olates [26] or phenolates [27] and fluorescent properties for imidazol-2-yl derivatives and their zinc complexes [33,34]. In further exploring the scope of using 2-((2-(*1H*-benzoimidazol-2-yl)quinolin-8-ylimino)methyl)phenol derivatives, which were initially developed as tetra-dentate ligands for aluminum complexes as pre-catalysts in polymerization applications [35], the zinc complexes have now been synthesized. The photoluminescent and fluorescent properties of both the organic compounds and their zinc complexes were investigated, revealing red-shifts occurred for zinc complexes as well as significant influences by the solvents used. Herein, the synthesis and characterization of the zinc complexes are reported as well as their photoluminescent behavior, which is compared to the ‘free-ligands’.

Results and Discussion

1. Synthesis and Characterization of Zinc Complexes C1 - C5

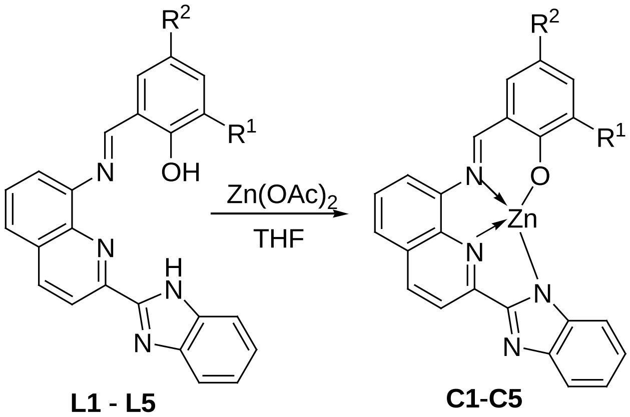

L1 - L5 **C1-C5**

Ln / Cn	L1 / C1	L2 / C2	L3 / C3	L4 / C4	L5 / C5
R^1	H	Me	^{t}Bu	Me	H
R^2	H	Me	^{t}Bu	^{t}Bu	Br

Scheme 1. Synthesis of ligands and their zinc complexes **C1-C5**

The series of 2-((2-(1H-benzo[d]imidazol-2-yl)quinolin-8-ylimino)methyl)phenol derivatives (**L1– L5**), synthesized according to our previous procedure [35], was reacted with a stoichiometric amount of $Zn(OAc)_2$ in THF to form the corresponding zinc complexes **C1–C5**, respectively. All zinc complexes were fully characterized by FT-IR spectroscopy and elemental analysis. Comparison of the IR spectra between the free organic compounds and their corresponding zinc complexes, reveals that the absorption between 3266-3330 cm^{-1} of $\nu_{(\text{-OH})}$ and 1613-1618 cm^{-1} for the $\nu_{(\text{N-H})}$ of the imidazole in the organic compounds (**L1–L5**) disappeared in the spectra of the zinc complexes **C1–C5**, indicating effective bond formation in the zinc complexes **C1–C5** (Scheme 1); the Zn-imidazolate bonds were formed by eliminating the proton of *N*-H within the complexes **C1–C5**, which contrasts with our previous observations for 2-(imidazol)phenolate zinc complexes where the N-H of imidazole remained [34]. The FT-IR spectra obtained for the **C2** re-crystallized in THF or CH_2Cl_2 were all the same, however, the spectrum observed was different when employing methanol, with an absorption at 1611 cm^{-1} for the $\nu_{(N\text{-}H)}$ of imidazole, indicating proton-migration from solvent into the imidazolate. Presumably due to H-bonding with the solvent - better to say this i think.

To confirm the molecular structure, the re-crystallization of complex **C2** was carried out in various solvents such as THF, dichloromethane, methanol, and chlorobenzene as well as the mixture solvents, however, single crystals suitable for the X-ray diffraction study were only obtained from methanol solution. As shown of complex **C2** in the Figure 1, the zinc is five-coordinated with the tetra-dentate ligand and a methanol binding at the zinc to form a distorted square-pyramid, in which the oxygen of the coordinated methanol occupies the vertex. The N, N, N, and O atoms of the tetra-dentate ligand are co-planar and provide the square base with the deviation distance of 0.353 Å within the pyramid,(deviation from what? The zinc from the base; or the N,N,N,O atoms from the plane?) which was similar to its aluminum analogues [35]. The bond length of Zn-$O_{phenolate}$ [1.9148(19) Å] is consistent to reported values for Zn-$O_{phenolate}$ [1.915(2)-1.946(2)], whilst the bond lengths of Zn-N [2.069(2), 2.184(2) Å] are slightly longer than those [1.953(3), 2.003(3) Å] in reported analogues (which analogues?) [25,34]. The Zn1-O2 2.072(2) Å indicated the single bonding cation-anion pair. ??

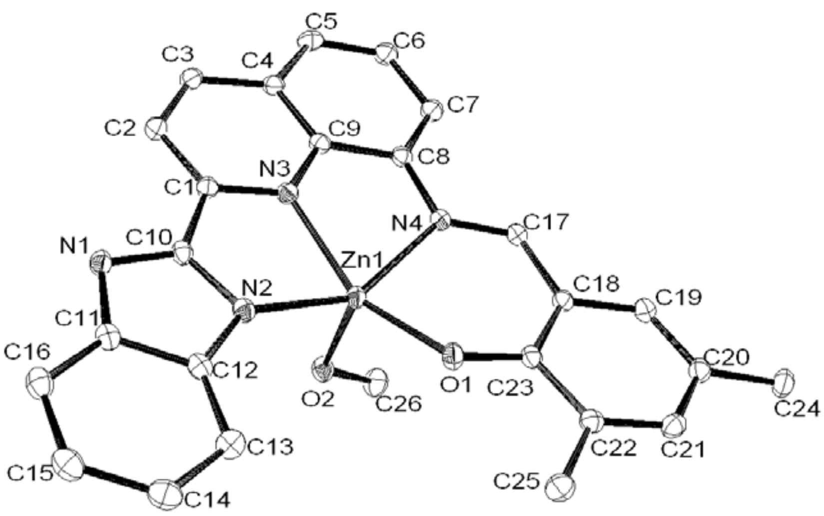

Figure 1 ORTEP drawing of **C2** with thermal ellipsoids drawn at the 30% probability level. Hydrogen atoms are omitted for clarity. Selected bond length (Å) and selected bond angles (°): Zn1-O1 1.9148(19), Zn1-N3 2.069(2), Zn1-O2 2.072(2), Zn1-N2 2.083(2), Zn1-N4 2.184(2), O1-Zn1-N3 154.17(9), O1-Zn1-O2 104.41(8), N3-Zn1-O2 97.78(8), O1-Zn1-N2 111.45(8), N3-Zn1-N2 77.11(9), O2-Zn1-N2 99.44(8), O1-Zn1-N4 89.34(8), N3-Zn1-N4 75.09(8), O2-Zn1-N4 96.26(8), N2-Zn1-N4 149.61(9), C23-O1-Zn1 129.69(17).

2. UV-Vis absorption spectra

The UV-Vis absorption spectra for the organic compounds and their zinc complexes were measured in various solvents with the concentration fixed at 2×10^{-5} M, and their data are tabulated in Table 1, revealing the characteristic differences of organic compounds and zinc complexes.

Table 1. The UV-Vis absorptions of organic compounds and their zinc complexes

solvent	Organic	$\lambda_{abs\text{-}max}$ (nm)	$\varepsilon_{(\lambda max)}$ ($M^{-1}.cm^{-1}$)	complex	$\lambda_{abs\text{-}max}$ (nm)	$\varepsilon_{(\lambda max)}$ ($M^{-1}.cm^{-1}$)
Methanol	**L1**	318	20600	**C1**	321	29600
THF		304	20100		329	29280
Dichloromethane		307	20070		327	27435
Toluene		308	18370		330	26245
Methanol	**L2**	323	36300	**C2**	325	31350
THF		307	34655		333	30500
Dichloromethane		309	35585		329	27810
Toluene		312	32360		332	19805
Methanol	**L3**	324	33050	**C3**	325	32850
THF		306	32060		333	31880
Dichloromethane		308	33100		329	29680
Toluene		310	29340		335	26690
Methanol	**L4**	323	23000	**C4**	324	28700
THF		306	23650		333	28075
Dichloromethane		308	22925		328	26220
Toluene		310	21355		334	22795
Methanol	**L5**	318	36600	**C5**	319	25500
THF		317	35680		330	24115
Dichloromethane		314	35325		324	23695
Toluene		317	34965		332	19945

2.1 Solvent effect on UV-absorption

2.2.1 UV-Vis absorption in methanol

Initially, we first compared the difference between **L2** and **C2** in methanol (Figure 2). In principle, both curves are very similar, but the complex displayed weaker absorption and a slight red shift, which is probably due to the interaction of intermolecular hydrogen bonds formed between the ligand (**L2**) and methanol and the coordination effect between metal and ligand.

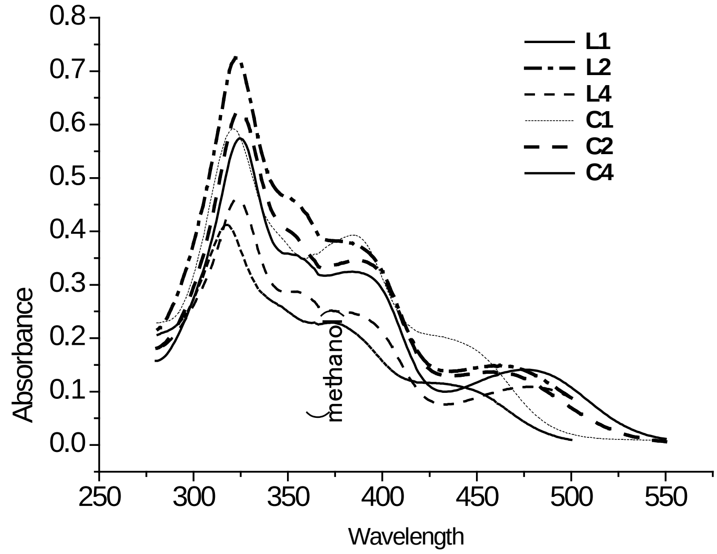

Figure 2 UV-vis absorption spectra of ligands (**L1**, **L2, L4)** and zinc complexes **(C1**, **C2, C4)** in methanol solution (2×10^{-5} M)

Figure 2 also reveals that the other ligands **L1, L4** in methanol have very similar UV-Vis absorption spectra when compared with their corresponding zinc complexes **C1, C4**, suggesting that similar phenomena occurred in their methanol solutions. In addition, the collected data in table 1 also revealed that in methanol, the $\lambda_{abs\text{-}max}$ (nm) of the ligands **L1-L5** is very close to that of the corresponding complexes **C1-C5**. For example, $\lambda_{abs\text{-}max}$ (nm) of **L1 (**318 nm**)** is close to that (321nm) of **C1** in methanol. The $\lambda_{abs\text{-} max}$ (nm) of the other ligands and complexes in methanol is 323 (**L2**) *vs* 325 (**C2**); 324(**L3**) *vs* 325 (**C2**), 323(**L4**) *vs* 324(**C4**) and 316(**L5**) *vs* 319 **(C5).** However, differences in absorption could be observed with different ligands and complexes. Combined with the X-ray structure of **C2** obtained from MeOH and the UV-Vis absorption spectra of the zinc complexes, proton-migration from methanol into the imidazolate was further proved. Isn't this just H-bonding?

2.2.2 UV-Absorption in other solvents (THF, CH_2Cl_2, Toluene)

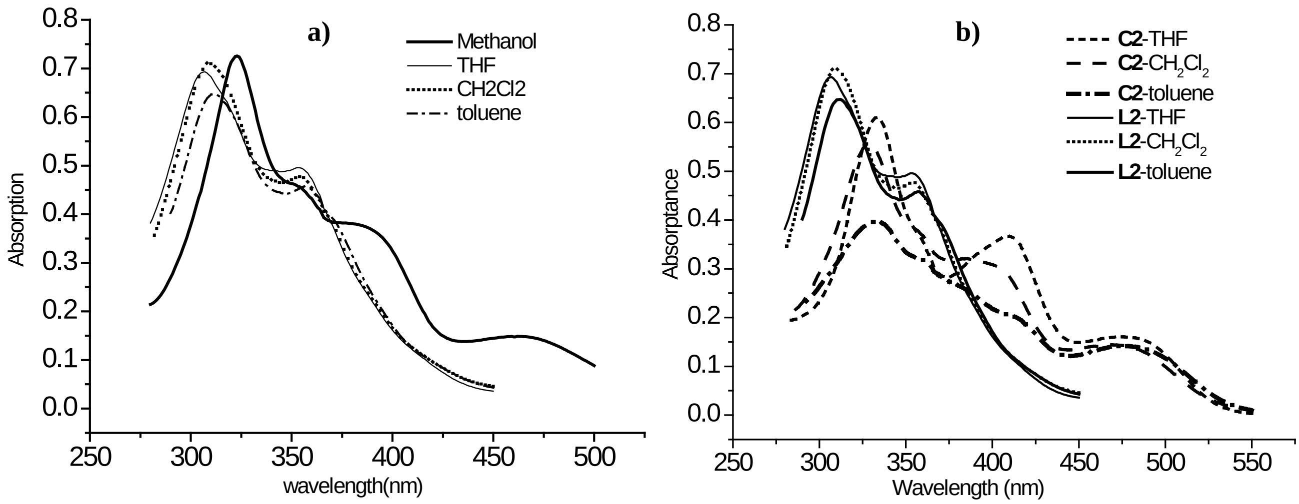

Figure 3 a) UV-Vis absorption spectra of **L2** in different solvents;

b) UV-Vis absorption of **C2** and **L2** in different solvents

Figure 3 reveals the solvent effects on the absorption of ligand **L2**. The absorption of **L2** in non-protic solvent such as toluene, CH_2Cl_2 and THF are significantly different to that in methanol, whilst all absorptions in non-protic solvents are very similar. The reason is probably due to hydrogen bonding between the N atom of the imidiazolyl or pyridyl rings in **L2** and the active proton of methanol, which causes the red shift of absorption wavelength compared with those in aprotic solvents. For example, the maximum absorption positions for **L2** appeared at 323 nm in methanol, 307 nm in THF, 309 nm in dichloromethane and 312 nm in toluene (Table 1). In methanol, the maximum absorption wavelength of the ligands were bathochromically shifted by about 14 nm compared to those in THF, which is attributed to the intermolecular and intramolecular hydrogen bonds between **L2** and methanol as reported previously [36, 37].

Comparing the spectra of **L2** with **C2** in other solvents (THF, CH_2Cl_2, Toluene, shown in figure 3b), generally it was found that significant red-shift occurred, due to the formation of a σ-bond between the Zn and the $N_{imidazol}$ atoms thereby extending the π-conjugated system. In contrast, there were no obvious shifts between **L2** and **C2** in methanol (figure 2), which is due to the hydrogen transfer in the protic solvent.

2.2. Ligand environment effects on the UV-absorption

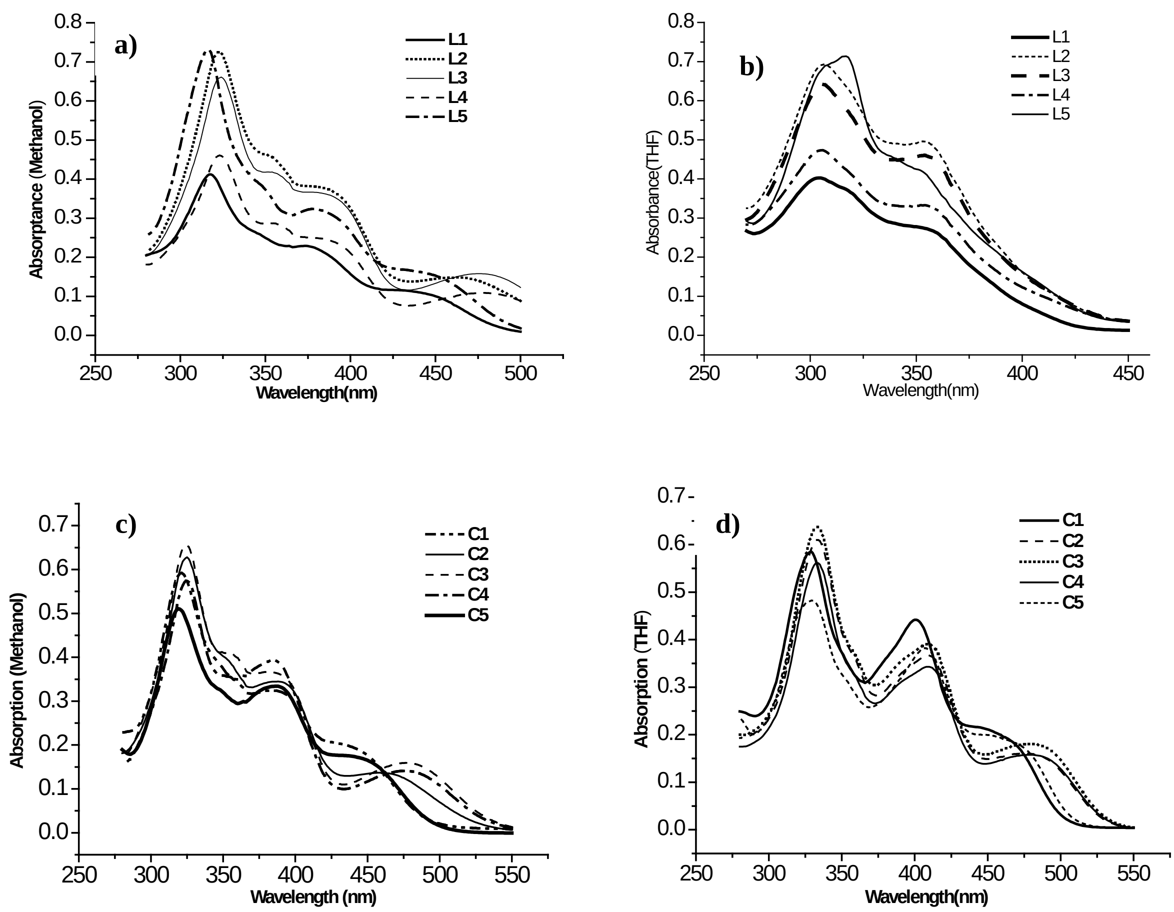

Figure 4 a) Absorption spectra of **L1–L**5 in CH_3OH; b) Absorption spectra of **L1–L**5 in THF; c) Absorption spectra of **C1–C**5 in CH_3OH; d) Absorption spectra of **C1–C**5 in THF

We also investigated the ligand environment effect on the absorption (shown in Figure 4). Very similar spectra for **L1-L5** and **C1-C5** in the same solvents were observed, such as CH_3OH and THF (Figure 4). This suggested that the substituents (R^1, R^2) on the phenolate had little effect on the absorption, probably due to their position, which is far from the π-conjugated system. For example, $\lambda_{abs\text{-}max}$ (nm) of absorption for **L1-L5** in CH_3OH is 318, 323, 324, 323, 318, while $\lambda_{abs\text{-}max}$ for complexes **C1-C5** in CH_3OH is found at 321, 325, 324, 325, 319 nm respectively, which are very similar to those of the ligands, further illustrating the methanol effect applies equally to all complexes. When the solvent is THF, $\lambda_{abs\text{-}max}$ (nm) of absorptions for ligands **L1-L5** are 304, 306, 307, 307, 316, whilst $\lambda_{abs\text{-}max}$ (nm) for the absorptions for complexes **C1-C5** are in the range 329-333 nm, showing a clear red-shift compared to that of ligands **L**1-**L5**.

Figure 4a, 4b shows that there are different intensity for absorptions with different ligands **L1-L5** in the same solvent, indicating the substituent effect on the UV-absorption. In contrast, only little differences were found in the intensity of the UV-absorption for **C1-C5 (**Figure 4c,d), which may be due to the coordination to the zinc center.

3. Fluorescence spectra in various solvents

The emission spectra of these ligands and their Zn^{2+} complexes were also measured in methanol, THF, dichloromethane, and toluene solution with a concentration of 2×10^{-5} mol/L at room temperature. The emission data for compounds **L1**−**L5** and **C1**−**C5** are collected in Table 2**.** It is interesting to observe that all ligands and complexes in various solvent exhibited large Stokes shifts (Table 2), which can be readily attributed to the excited-state intramolecular proton-transfer (ESIPT) phenomenon and the photo-excitation of the closed *cis*-enol form that resulted in generation of the excited state keto form (Scheme 3). Compared with the $\Delta\lambda^a$ of the ligands **L1-L5**, the Stokes shift of the zinc complexes **C1-C5** in most cases increased upon coordination (Table 2).

Table 2 Emission data for compounds **L1**−**L5** and **C1**−**C5**

media	Ligands				Complexes		
		λ_{maxEm} (nm)	λ_{Ex} (nm)	$\Delta\lambda^a$ (nm)		λ_{maxEm} (nm)	λ_{Ex} (nm)	$\Delta\lambda^a$ (nm)
Methanol	**L1**	540	380	160	**C1**	552	380	172
THF		509	380	129		539	380	159
CH_2Cl_2		525	380	145		542	380	162
Toluene		505	380	125		539	380	159
Methanol	**L2**	543	380	163	**C2**	563	380	183

THF		508	380	128		568	380	188
CH_2Cl_2		523	380	143		572	380	192
Toluene		505	380	125		567	380	187
Methanol	**L3**	545	380	165	**C3**	572	380	192
THF		509	380	129		566	380	186
CH_2Cl_2		523	380	143		572	380	192
Toluene		506	380	126		565	380	185
Methanol	**L4**	543	380	163	**C4**	570	380	190
THF		508	380	128		567	380	187
CH_2Cl_2		520	380	140		573	380	193
Toluene		503	380	123		565	380	185
Methanol	**L5**	544	380	164	**C5**	550	380	170
THF		509	380	129		532	380	152
CH_2Cl_2		522	380	142		540	380	160
Toluene		505	380	125		537	380	157

[a] $\Delta\lambda$ = Stokes shift

\

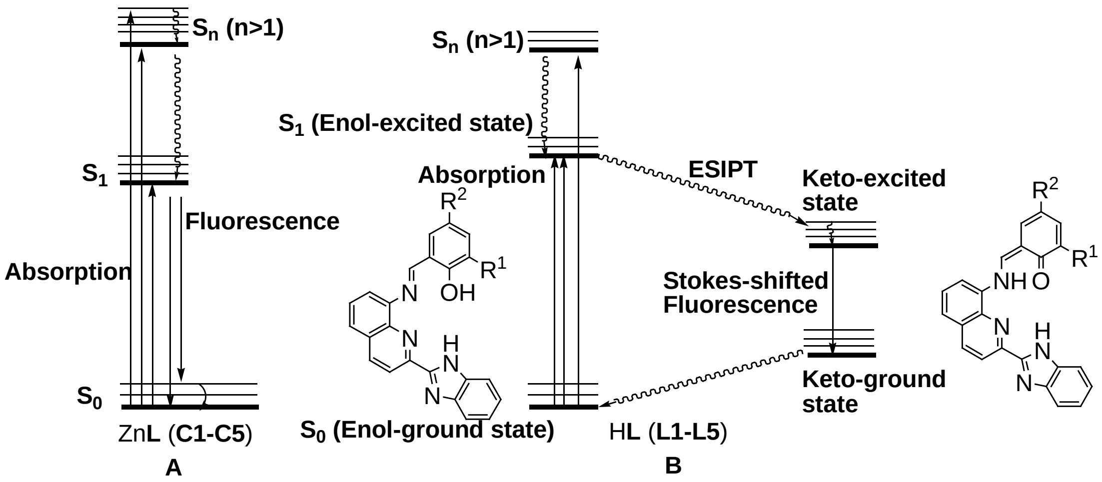

Scheme 3 Electronic transitions in the photo-luminescent process for zinc complexes (A) and ligands (B)

The solvent also had a large effect on the wavelength of the emission peaks. For all the ligands **L1-L4**, λ_{maxEm}(nm) and $\Delta\lambda^a$ increased with solvent polarity, as demonstrated by the order: methanol > CH_2Cl_2 > THF > toluene. For the complexes **C1-C5**, although the λ_{maxEm} and $\Delta\lambda^a$ were synchronously? affected by solvent, the order was very different to that for ligands in different solvent. This is because their excited states possess a larger dipole moment than that of corresponding ground states.

In addition, the ligand environment also had a big effect on the fluorescence spectra. Figure 5 shows the fluorescence spectra of ligands **L1-L5** in different solvents. The emission intensities and quantum yield of **L5** are much higher than those of **L1-L4** in methanol and CH_2Cl_2, and decreased in the order: **L5** (H, Br) > **L1** (H, H) > **L2** (Me, Me) > **L3** (^{t}Bu, ^{t}Bu) > **L4** (Me, ^{t}Bu) (Table 3), which can be explained in terms of an electron effect. The electron-donating substituent on the phenol ring can push electrons into the delocalized π-system and decreased the electron density and stability of the more extensive π-conjugated systems in **L2**, **L3** and **L4**, thereby enhancing the photo-induced electron transfer (PET), which would allow for a non-radiative decay pathway from the fluorescent moiety and decrease the fluorescence intensity and quantum yield. In particular, the fluorescence intensity and quantum yield of **L5** (H, Br) are much higher than the others (**L1-L4**), which is probably due to the electron affinity of Br atom that will weaken the non-radiative decay and enhance the p-π delocalized bonding formed between Br and other group which? [34]. The fluorescence spectra in other solvents such as THF, dichloromethane, toluene also showed the highest intensity for **L5** and the lowest intensity for **L4** (Figure 5).

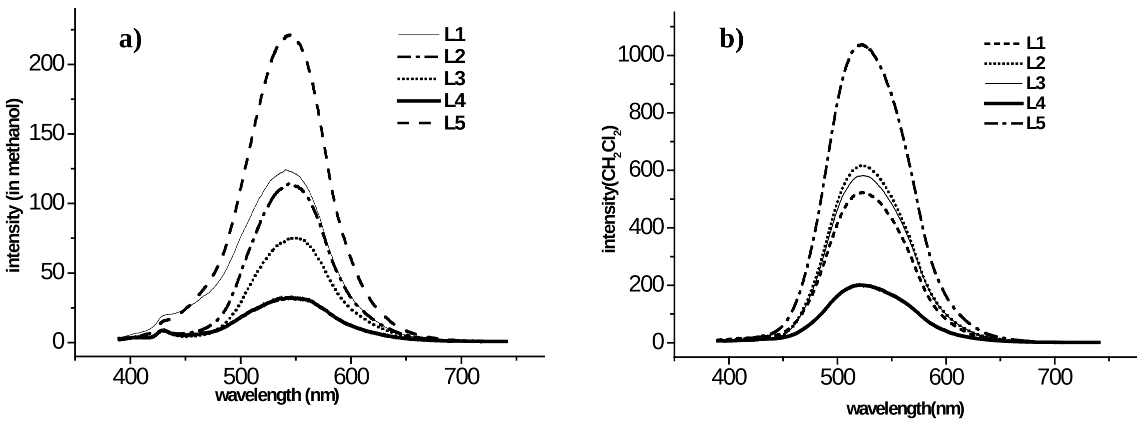

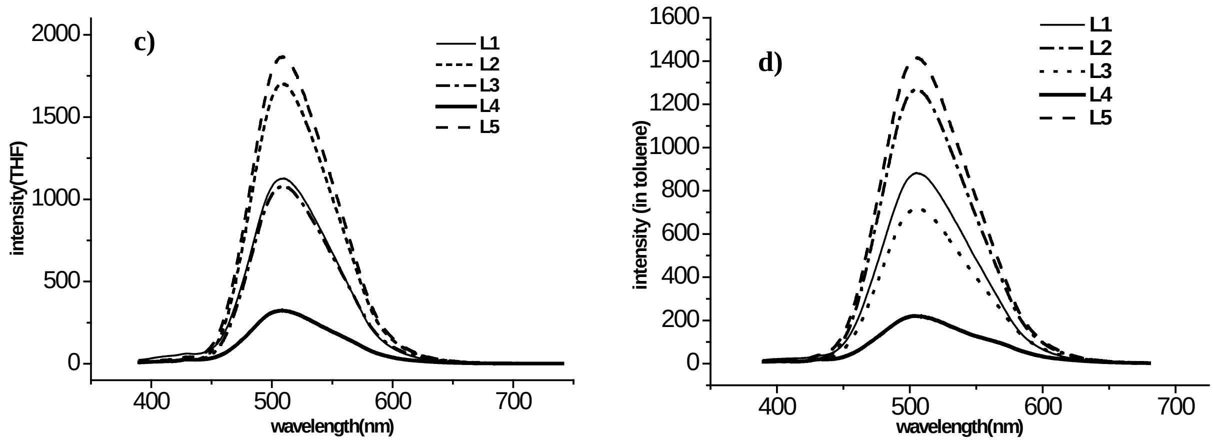

Figure 5 Fluorescence spectra of ligands **L1-L5** in different solvents (2×10^{-5} mol/L) a) methanol; b) THF; c) dichloromethane; d) toluene.

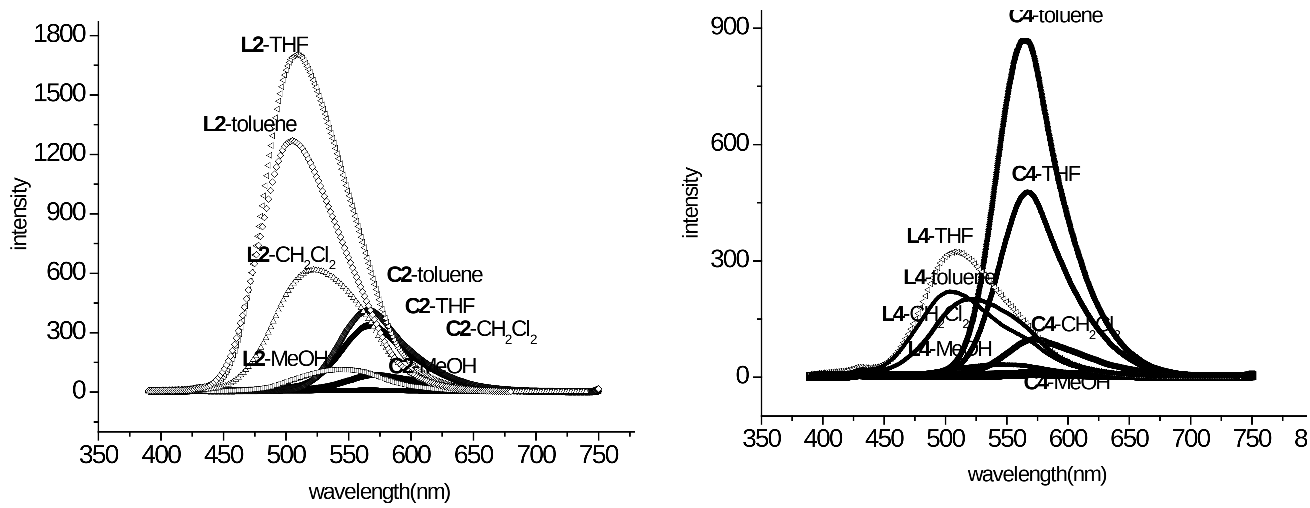

Figure 6 Fluorescence spectra of ligands (**L2, L4**) and zinc complexes (**C2**, **C4**) in solution (2×10^{-5} mol/L) of methanol, THF, dichloromethane and toluene.

Figure 6 clearly showed that the emission bands of zinc complexes **C2, C4** were red-shifted compared with the corresponding ligands **L2** and **C4** in different solvents. In order to rationalize the factors responsible for these red-shifted fluorescence spectra, the electronic perturbation of the complexes should be mentioned. These emissions observed in Zn^{2+} complexes are neither metal-to-ligand charge transfer (MLCT) nor ligand-to-metal charge transfer (LMCT) in nature, because the zinc ion is quite a stable species due to the d^{10} configuration [38]. Thus, the emission can be assigned to the ligand-centered $\pi \rightarrow \pi^*$ excitation [39]. Due to the coordination of the zinc ion to the 'free' ligand, both the π and π^* orbital energy decreased, which led to the red-shift of the emission of the chelated ligand. The fluorescence intensity of the zinc complexes exhibited either a higher or a lower intensity than did their corresponding ligands. These changes could be explained by the solvent effects and the intra-ligand charge-transfer (ILCT).

The fluorescence lifetimes were measured and the calculated radiative (kr) values of ligands and zinc complexes are summarized in Table 3. The results showed that most of the fluorescence decay of the ligands and zinc complexes followed a double exponential decay in various solvents, except for several cases where there is a single exponential decay, such as for **L1**, **C1** and **C5** in methanol, **C2**, **C3** in THF, and **C4** in THF and toluene (Table 3). The reason for two different lifetimes could be explained by different excited state species that occur from slower conversion rates for the two species than the emission rate, which also suggested that these species were not in equilibrium [40]. In other words, when the fluorescence decay followed a single exponential, there was one kind of species present in solvent. The double exponential decay symbolizes there are two kinds of emission species existing in solution [41].

Table 3 Excited singlet state lifetimes (ns) and the values of radiative decay rate (kr) of ligands (**L1**−**L5**) and zinc complexes (**C1**−**C5**).

Media		Ligands						Complexes				
		Φ_F	τ_1 (ns)	k_{r1}^a ($10^6 s^{-1}$)	τ_2 (ns)	k_{r2}^a ($10^6 s^{-1}$)		Φ_F	τ_1 (ns)	k_{r1}^a ($10^6 s^{-1}$)	τ_2 (ns)	k_{r2}^a ($10^6 s^{-1}$)
Methanol	**L1**	0.0623	1.39	44.82	-	-	**C1**	0.0965	1.541	62.63	-	-
THF		0.7169	7.719	92.88	1.426	502.76		0.2342	3.186	73.49	1.205	194.3
CH_2Cl_2		0.3387	0.446	757.8	7.561	44.94		0.0976	0.5966	163.6	3.799	25.69

Toluene		0.5673	0.616	921.2	4.866	116.6		0.1429	0.6292	227.0	4.266	33.49
Methanol	**L2**	0.0289	2.475	11.72	0.413	70.21	**C2**	0.0049	0.3557	14.00	2.99	1.665
THF		0.5744	2.356	243.8	8.450	67.98		0.1032	3.15	32.76	-	-
CH_2Cl_2		0.2315	0.452	511.4	4.311	53.69		0.0284	1.191	23.85	4.175	6.804
Toluene		0.4441	0.434	1022	4.923	90.21		0.1491	5.365	27.79	4.073	36.62
Methanol	**L3**	0.0203	0.359	56.56	3.432	5.928	**C3**	0.0037	0.3566	10.36	2.95	1.252
THF		0.3986	1.095	364.0	5.047	78.98		0.1477	3.807	38.78	-	-
CH_2Cl_2		0.2403	0.381	630.8	5.120	46.93		0.0305	1.195	25.58	5.981	5.111
Toluene		0.2855	0.418	682.4	4.365	65.41		0.2531	6.484	39.03	4.380	57.78
Methanol	**L4**	0.0157	0.3347	46.87	3.408	4.603	**C4**	0.0043	0.3121	13.85	2.984	1.448
THF		0.1721	0.7992	215.3	4.217	40.80		0.1462	3.806	38.41	-	-
CH_2Cl_2		0.1270	0.4245	299.2	4.8	26.46		0.0335	1.170	28.65	3.751	8.937
Toluene		0.1370	0.4471	306.5	4.598	29.80		0.2956	4.44	66.59	-	-
Methanol	**L5**	0.0688	1.46	47.17	3.957	17.41	**C5**	0.1611	1.529	105.3	-	-
THF		0.7284	1.322	550.9	10.28	70.85		0.2920	1.354	215.7	3.457	84.03
CH_2Cl_2		0.4622	0.5662	816.4	6.211	74.42		0.0742	0.4398	168.7	3.176	23.35
Toluene		0.6182	0.7536	820.3	4.598	134.4		0.1507	0.515	292.6	3.962	38.03

Concentration: 2×10^{-5} M. a: $k_r = \Phi_F/\tau$,

Conclusion

A series of 2-((2-(1H-benzo[d]imidazol-2-yl)quinolin-8-ylimino)methyl)phenols (**L1**– **L5**) and the zinc complexes (**C1**– **C5**) thereof were synthesized and fully characterized. A crystal structure of **C2** was determined by X-ray diffraction and revealed that hydrogen immigration from methanol to imidazole group – what about using CD_3OH and seeing is there is a shift in the IR!

The different UV-absorption of the ligands **L1-L5** and complexes **C1-C5** in methanol and other solvents further demonstrated this observation. Due to the ESIPT phenomenon and coordination effect, the ligand and complexes exhibited large Stokes shifts. The fluorescent intensities of the zinc complexes were also greatly affected by the substituents at the phenolic ring. In addition, most of the fluorescence decay followed a double exponential decay in various solvents, except for a single exponential decay in some cases.

Experiment

1. General Information.

The ^{1}H and ^{13}C NMR spectra were recorded on a Bruker DMX 400 MHz instrument at ambient temperature using tetramethylsilane (TMS) as an internal standard at 25 ºC. FT-IR spectra of the ligands (**L1-L5**) and corresponding Zn complexes (**C1-C5**) which were dried under vacuum at 60 ºC for 24 h were recorded on a Perkin Elmer FT-IR 2000 spectrometer using KBr disc in the range of 4000–400 cm^{-1}. Elemental analyses were performed on a Flash EA 1112 microanalyzer. The steady-state fluorescent spectra were measured on an F4500-FL fluorescence spectrophotometer and the excitation slit was 5 nm; fluorescence lifetimes were obtained using the time-correlated single-photon counting technique (Edinburgh Analytical Instruments F900 fluorescence spectrofluorimeter).

2. Calculation of fluorescence quantum yield.

Fluorescence quantum yield measurements were carried out on a F4500-FL fluorescence spectrometer. The fluorescence quantum yield for samples in solution was measured by using the solution containing coumarin 307 in methanol (Φ = 0.56) standard as the reference, Φ was calculated according to the following equation:

$$\Phi_s = \Phi_r \left(\frac{A_r(\lambda_r)}{A_s(\lambda_s)} \right) \left(\frac{I(\lambda_r)}{I(\lambda_s)} \right) \left(\frac{n_s^2}{n_r^2} \right) \frac{\int F_s}{\int F_r}$$

Where *r* represents the standard, *s* represents the samples, *Ar (λr)* and *As (λs)* are the respective absorbance of the standard and the measured samples, *I (λr)* and *I (λs)* are the respective emission intensities of the standards and samples, *n* is the refractive index of the corresponding solvents, ∫F is the integral area of one-photon fluorescence, and Φ represents the fluorescence quantum yield.

3. Synthesis of ligands L1-L5 and zinc complexes C1-C5

3.1 Synthesis of 2-(1H-benzo[d]imidazol-2-yl)quinolin-8-amine. The mixture of

2-methylquinolin-8-amine (16.9 g, 100 mmol) and benzene-1,2-diamine (10.8 g, 100 mmol) was heated to 170 ℃ in the presence of elemental sulfur (32 g, 1 mol) for 12 h to afford the crude product. The resultant mixture was cooled and then was extracted by dichloromethane, the collected solution were removed all of solvent and the residue were purified by column chromatography on silica gel with petroleum ether/ethyl acetate (3/1, v/v) as eluent to afford the product as a yellow powder in 23.5 % (6.41 g, 23.5 mmol) yield. ^{1}H NMR (400 MHz, $CDCl_3$, TMS): δ 10.57 (s, 1H); 8.51 (d, J = 8.8, 1H); 8.22 (d, J = 8.8, 1H); 7.70-7.85 (m, 2H); 7.38 (t, J = 7.6, 1H); 7.30-7.37 (m, 2H); 7.22 (d, J = 7.2, 1H); 6.99 (d, J = 6.4, 1H) 5.1(s, 2H). ^{13}C NMR (100 MHz, $CDCl_3$, TMS): δ 151.4, 148.7, 145.4, 143.9, 138.4, 137.6, 137.4, 135.4, 129.3, 128.4, 125.1, 119.3, 117.0, 116.3, 113.0, 111.0. IR (KBr; cm^{-1}): ν 3463, 3359, 3044, 2162, 1980, 1899, 1811, 1770, 1612, 1583, 1444, 1429, 1274, 1223, 1116, 1012, 980, 836, 666. Anal.calcd for $C_{16}H_{12}N_4O$: C 73.83, H 4.65, N 21.52. Found: C 73.15, H 4.12, N 21.23 %.

3.2 2-(2-(1H-benzoimidazol-2-yl)quinolin-8-yliminomethyl)phenol (L1). 1H-benzo[d]imidazol-2-yl)quinolin-8-amine (0.518 g, 2.0 mmol), 2-hydroxybenzaldehyde (0.244 g, 2.0 mmol) and a few drops of acetic acid were refluxed in ethanol (20 ml) for 24 h, whereupon the crude product precipitated as a red powder from the reaction solution. After filtering and washing with 10 ml of ethanol for three times, the pure product (0.37 g, 1.02 mmol) was obtained as red powder in yield 50.8%. ^{1}H NMR (400 MHz, $CDCl_3$, TMS): δ 16.15 (s, 1H), 11.18 (s, 1H), 8.94 (s, 1H), 8.58 (d, J = 8.4, 1H), 8.33 (d, J = 8.4, 1H), 7.89 (d, J = 7.6, 1H), 7.81 (d, J = 8.0, 1H), 7.60-7.72 (m, 3H), 7.46-7.50 (m, 2H), 7.21-7.39 (m, 2H), 7.19 (d, J = 8.4, 1H), 6.94-6.98 (m, 1H). ^{13}C NMR (100 MHz, $CDCl_3$, TMS): δ 155.8, 143.4, 142.9, 137.4, 137.3, 136.2, 126.9, 126.8, 126.7, 126.5, 122.2, 114.5, 106.2, 25.4, 24.9, 15.0. IR (KBr; cm^{-1}): ν 3263, 3053, 1618, 1590, 1505, 1434, 1315, 1272, 1226, 1150, 1004, 835, 734. Anal.calcd for $C_{23}H_{16}N_4O$: C 75.81, H 4.43, N 15.38. Found: C

75.82, H 4.04, N 15.33 %.

3.3 2-(2-(1H-benzoimidazol-2-yl)quinolin-8-yliminomethyl)-4,6-dimethylphenol (L2). The same procedure as preparing **L1** was used to synthesize **L2**, but 2-hydroxy-3,5-dimethylbenzaldehyde (0.3 g, 2.0 mmol) and 2-(1H-benzo[d]imidazol-2-yl)quinolin-8-amine (0.518 g, 2.0 mmol) were used. The red powder **L2** (0.48 g, 1.23 mmol) was isolated in 61.4 % yield. ^{1}H NMR (400 MHz, $CDCl_3$, TMS): δ 16.89 (s, 1H); 11.61 (s, 1H); 8.87 (s, 1H); 8.57 (d, *J* = 8.0, 1H); 8.33 (d, *J* = 8.4, 1H); 7.91 (d, *J* = 7.6, 1H); 7.32-7,79 (m, 2H); 7.63 (t, *J* = 8.0, 2H); 7.34-7.39 (m, 2H); 7.21 (s, 1H); 7.11 (s, 1H); 2.54 (s, 3H); 2.34 (s, 3H). ^{13}C NMR (100 MHz, DMSO, TMS): δ 197.3, 157.2, 151.8, 146.4, 144.9, 139.1, 137.4, 136.9, 130.8, 129.2, 128.7, 126.2, 120.8, 118.8, 113.5, 109.3, 55.4, 20.2, 15.3. IR (KBr; cm^{-1}): ν 3341, 3054, 2910, 2166, 2032, 1618, 1559, 1437, 1310, 1222, 1158, 1031, 719, 839, 791, 677. Anal.calcd for $C_{25}H_{20}N_4O$: C 75.51, H 5.14, N 14.20. Found: C 75.49, H 5.13, N 14.14 %.

3.4 2-(2-(1H-benzoimidazol-2-yl)quinolin-8-yliminomethyl)-4,6-di-*tert*-butylphenol (L3). The same procedure was used to synthesize **L3**, but 3,5-di-*tert*-butyl-2-hydroxybenzaldehyde (0.47 g, 2.0 mmol) and 2-(1H-benzo[d]imidazol-2-yl)quinolin-8-amine (0.518 g, 2.0 mmol) was used. The red powder **L3** (0.2 g, 0.42 mmol) was isolated in 21.0 % yield. ^{1}H NMR (400 MHz, $CDCl_3$, TMS): δ 16.89 (s, 1H); 11.18 (s, 1H); 8.98 (s, 1H); 8.57 (d, *J* = 8.54, 1H); 8.32 (d, *J* = 8.57, 1H); 7.90 (d, *J* = 7.86, 1H); 7.75 (m, 2H); 7.69 (d, *J* = 7.86, 1H); 7.61 (t, *J* = 7.80, 1H); 7.55 (d, *J* = 2.14, 1H); 7.31-7.40 (m, 2H); 7.29 (d, *J* = 2.14, 1H); 1.71 (s, 9H); 1.38 (s, 9H). ^{13}C NMR (100 MHz, $CDCl_3$, TMS): δ 163.64; 159.42; 151.13; 147.77; 141.71; 141.57; 139.82; 138.37; 137.06; 129.36; 129.18; 127.37; 126.39; 126.06; 124.47; 122.76; 120.43; 119.59; 118.36; 114.85; 111.75; 35.59; 34.31; 31.47; 31.39; 29.91; 29.35. IR (KBr; cm^{-1}): ν 3330, 3045, 2951, 2903, 2864, 1618, 1596, 1505, 1464, 1445, 1411, 1314, 1226, 846, 764, 731. Anal.calcd for $C_{31}H_{32}N_4O$: C 78.12, H 6.77, N 11.76. Found: C

77.99, H 7.04, N 11.32 %.

3.5 2-(2-(1H-benzoimidazol-2-yl)quinolin-8-yliminomethyl) -4-*tert*-butyl-6- methylphenol (L4). The same procedure was used to synthesize **L4**, but 5-*tert*-butyl-2-hydroxy-3-methylbenzaldehyde (0.38 g, 2.0 mmol) and 2-(1H-benzo[d]imidazol-2-yl)quinolin-8-amine (0.518 g, 2.0 mmol) were used. The red powder **L4** (0.35 g, 0.81 mmol) was isolated in 40.4 %yield. ^{1}H NMR (400 MHz, $CDCl_3$, TMS): δ 16.85 (s, 1H), 11.17 (s, 1H), 8.88 (s, 1H), 8.57 (d, J = 8.4, 1H), 8.30 (d, J = 8.4, 1H), 7.90 (d, J = 8.0, 1H), 7.68-7.76 (m, 3H), 7.59 (t, J = 7.6, 1H), 7.32-7.40 (m, 2H), 7.28 (d, J = 2.0, 1H), 7.10 (s, 1H), 2.35 (s, 3H), 1.69 (s, 9H). ^{13}C NMR (100 MHz, DMSO): δ 198.5, 157.8, 151.3, 145.8, 144.4, 136.8, 136.4, 134.9, 131.7, 128.6, 127.9, 120.3, 118.3, 112.9, 108.7, 54.8, 34.5, 34.2, 29.3, 28.9, 19.9. IR (KBr; cm^{-1}): ν 3320, 2948, 2911, 1614, 1505, 1437, 1351, 1311, 1230, 1007, 834, 726, 676. Anal.calcd for $C_{28}H_{26}N_4O$: C 77.39, H 6.03, N 12.89. Found: C 77.35, H 6.18, N 12.88 %.

3.6 2-(2-(1H-benzo[d]imidazol-2-yl)quinolin-8-yliminomethyl)-4-bromophenol (L5). The same procedure was used to synthesize **L5**, but 5-bromo-2-hydroxybenzaldehyde (0.40 g, 2.0 mmol) and 2-(1H-benzo[d]imidazol-2-yl)quinolin-8-amine (0.518 g, 2.0 mmol) were used. The red powder **L5** (0.45 g, 1.04 mmol) was isolated in 51.9 % yield. ^{1}H NMR (400 MHz, DMSO, TMS): δ 10.99 (s, 1H), 10.22 (s, 1H), 7.64-7.73 (m, 4H), 7.07-7.10 (m, 1H), 6.99 (d, J = 8.0, 1H), 6.89 (d, J = 8.0, 1H), 6.52 (s, 1H). ^{13}C NMR (100 MHz, DMSO, TMS): 190.3, 182.7, 160.4, 156.6, 151.9, 150.1, 146.4, 145.1, 142.5, 139.0, 137.5, 137.1, 134.3, 131.1, 139.3, 124.6, 120.5, 118.9, 113.6, 111.3, 109.4, 55.5. IR (KBr; cm^{-1}): ν 3312, 3045, 1613, 1467, 1403, 1312, 1272, 1182, 1117, 1042, 819, 756, 672. Anal.calcd for $C_{23}H_{15}BrN_4O$: C 62.32, H 3.41, N 12.64. Found: C 61.52, H 3.37 N 12.49 %.

3.7 (2-((2-(1H-benzo[d]imidazol-2-yl)quinolin-8-ylimino)methyl)phenoxylate zinc complex (C1). **L1** (0.15 g, 0.41 mmol) was dissolved in the mixture of THF (20 ml) and ethanol (10 ml) solution, then zinc acetate dihydrate (0.09 g, 0.41 mmol) was added and the mixture changed into a clear solution. After stirring 12 h at room temperature, a yellow precipitate were observed which was filtered and dried *in vacuo* to afford complex **C1** in 68.2 % (0.12 g, 0.28 mmol) yield. IR (KBr; cm^{-1}): ν 3049, 2165, 2030, 1978, 1570, 1523, 1442, 1413, 1323, 1192, 1143, 1121, 1075, 914, 839. Anal.calcd for $C_{23}H_{14}N_4OZn$: C 64.58, H 3.30, N 13.10. Found: C 64.15, H 3.40 N 12.69 %.

3.8 (2-((2-(1H-benzo[d]imidazol-2-yl)quinolin-8-ylimino)methyl)-4,6-dimethyl phenoxylate zinc complex (C2). The same procedure with **C1** was used to synthesize **C2**, but **L2** (0.108 g, 0.28 mmol) was used instead of **L1**, and reacted with zinc acetate dihydrate (0.065 g, 0.28 mmol) in THF (20 ml) and ethanol (10 ml) solution. The residue **C2** was isolated in 95.7 % (0.12 g, 0.26 mmol) yield. IR (KBr; cm^{-1}): ν 3057, 2394, 2285, 1879, 1534, 1505, 1412, 1384, 1320, 1244, 1217, 1168, 966, 854, 748, 669. Anal.calcd for $C_{25}H_{18}N_4OZn$: C 65.87, H 3.98, N 12.29. Found: C 65.45, H 4.23, N 12.21 %. In order to demonstrate the regeneration of hydrogen of N_{imidzaol}-H, the C2 was dissolved in methanol, then the solvent was removed to obtain the product that was used to measure above IR spectra: IR (KBr; Methanol; cm^{-1}): ν 2960, 2921, 2852, 1724, 1611, 1538, 1420, 1320, 1257, 1217, 1013, 851, 794, 745, 700.

3.9 2-((2-(1H-benzo[d]imidazol-2-yl)quinolin-8-ylimino)methyl)-4,6-di-*tert*-butylphenoxylate zinc complex (C3). The same procedure with **C1** was used to synthesize **C3**, but **L3** (0.1 g, 0.21 mmol) was used instead of **L1**, and reacted with zinc acetate dihydrate (0.046 g, 0.21 mmol) in THF (20 ml) and ethanol (10 ml) solution. The residue **C3** (0.06 g, 0.11 mmol) was isolated in 53.0 % yield. IR (KBr; cm^{-1}): ν 2904, 2535, 2166, 2031, 1527, 1414, 1382, 1341, 1319, 1225, 1154, 969, 930, 855, 749, 666. Anal.calcd for $C_{31}H_{30}N_4OZn$: C 68.95, H 5.60, N 10.38. Found: C 68.92, H 5.53 N 10.11 %.

3.10 2-((2-(1H-benzo[d]imidazol-2-yl)quinolin-8-ylimino)methyl)-4-*tert*-butyl-6- methyl phenoxylate zinc complex (C4). The same procedure as **C1** was used to synthesize **C4**, but **L4** (0.1

g, 0.22 mmol) was used instead of **L1**, and reacted with zinc acetate dihydrate (0.05 g, 0.22 mmol). The residue **C4** (0.048 g, 0.01 mmol) was isolated in 43.8 % yield. IR (KBr; cm^{-1}): ν 2902, 2635, 1526, 1504, 1380, 1317, 1224, 1154, 1077, 968, 930, 851, 744, 664. Anal.calcd for $C_{28}H_{24}N_4OZn$: C 67.54, H 4.86, N 11.25. Found: C 67.15, H 5.08 N 11.11 %.

3.11 ((2-(1H-benzo[d]imidazol-2-yl)quinolin-8-ylimino)methyl)-4-bromo-phenoxylate zinc complex (C5). The same procedure as **C1** was used to synthesize **C5**, but **L5** (0.22 g, 0.5 mmol) was used instead of **L1**, and reacted with zinc acetate dihydrate (0.11 g, 0.5 mmol) in THF (20 ml) and ethanol (10 ml) solution. The residue **C5** (0.21 g, 0.42 mmol) was isolated in 84.7 % yield. IR (KBr; cm^{-1}): ν 2969, 2868, 1569, 1507, 1442, 1378, 1315, 1274, 1229, 1174, 1151,1133, 1053, 840, 822, 745. Anal.calcd for $C_{23}H_{13}BrN_4OZn$: C 54.52, H 2.95, N 11.06. Found: C 54.31, H 2.79 N 10.61 %.

4. X-ray crystallographic studies

Single crystals of complex **C2** suitable for X-ray diffraction were grown by the slow diffusion of *n*-hexane into each methanol solution. Crystallographic data of compound **C2** are summarized in Table1. X-ray studies were carried out on a Rigaku Saturn 724+ CCD with graphite-monochromatic Mo Kα radiation (k = 0.71073 Å) at 173 (2) K, cell parameters were obtained by global refinement of the positions of all collected reflections. Intensities were corrected for Lorentz and polarization effects and empirical absorption. The structures were solved by direct methods and refined by full-matrix leasts squares on F^2. All hydrogen atoms were placed in calculated positions. Structure solution and refinement were performed by using the SHELXL-97 package [42]. Crystal data and processing parameters for complexes **C2** are summarized in Table 4.

Table 4 Crystal data and structure refinement for **C2**

	C2

Empirical formula	$C_{26}H_{19.50}N_4O_2Zn$
fw	485.33
T/K	173(2)
λ/ Å	0.71073
Cryst. syst.	Monoclinic
Space group	P2(1)/c
a/ Å	11.633(2)
b/ Å	23.038(5)
c/ Å	8.5929(17)
α (°)	90.00
β (°)	111.41(3)
γ (°)	90.00
V (Å^3)	2144.0(7)
Z	4
Dcalcd. (Mgcm^{-3})	1.504
μ/ mm^{-1}	1.178
F(000)	998
Cryst. size / mm	0.44 x 0.18 x 0.06
θ range (°)	2.08 to 27.51 deg
Limiting indices	-15<=h<=10, -29<=k<=29, -11<=l<=10
No. of rflns collected	15923
No. unique rflns [*R*(int)]	4861 [R(int) = 0.0633]
Completeness to θ (%)	98.8 %
Abs corr	None
Data / restraints / params	4861 / 408 / 298
Goodness of fit on F^2	1.120
Final *R* indices[$I > 2\sigma(I)$]	R1 = 0.0515, wR2 = 0.1159

R indices (all data)	R1 = 0.0607, wR2 = 0.1199
Largest diff. peak and hole (e Å^{-3})	0.569 and -0.668

Acknowledgement

Reference

[1] A. P. de Silva, H. Q. N. Gunaratne, T. Gunnlaugsson, A. J. M. Huxley, C. P. McCoy, J. T. Rademacher, T.E. Rice, Signaling Recognition Events with Fluorescent Sensors and Switches, *Chem. Rev.* 97 (1997)1515-1566.

[2] P. J. Stang, B. Olenyuk, Self-Assembly, Symmetry, and Molecular Architecture: Coordination as the Motif in the Rational Design of Supramolecular Metallacyclic Polygons and Polyhedra, *Acc. Chem. Res.* 30 (1997) 502-518.

[3] K.E. Erkkila, D.T. Odom, J.K. Barton, Recognition and Reaction of Metallointercalators with DNA , *Chem. Rev.* 99 (1999) 2777-2795.

[4] M. Irie, T. Fukaminato, T. Sasaki, N. Tamai, T. Kawai, A digital fluorescent molecular photoswitch, *Nature* 420 (2002) 759-760.

[5] W. M. Leevy, S.T. Gammon, H. Jiang, J. R. Johnson, D. J. Maxwell, E. N. Jackson, M. Marquez, D. Piwnica-Worms, B. D. Smith, Optical Imaging of Bacterial Infection in Living Mice Using a Fluorescent Near-Infrared Molecular Probe , *J. Am. Chem. Soc.* 128 (2006) 16476-16477.

[6] E. I. Yslas, E. N. Durantini, V. A. Rivarola, Zinc-(II) 2, 9, 16, 23-tetrakis (methoxy) phthalocyanine: Potential photosensitizer for use in photodynamic therapy *in vitro*, *Bioorg. Med.*

Chem. 15 (2007) 4651-4660.

[7] C. Frederickson, Neurobiology of Zinc and Zinc-Containing Neurous, *J. Int. Rev. Neurobiol.* 31 (1989) 145-238.

[8] J. M. Berg, Y. Shi, The Galvanization of Biology: A Growing Appreciation for the Roles of Zinc, *Science* 271 (1996) 1081-1085

[9] A. E. Majzoub, C. Cadiou, I. Déchamps-Olivier, B. Tinant, F. Chuburu, Zinc(II) and PPi Selective Fluorescence OFF-ON-OFF Functionality of a Chemosensor in Physiological Conditions, *Inorg. Chem.* 50 (2011) 4029–4038.

[10] M. M. Yu, Z. X. Li, L. H. Wei, D. H. Wei, M. S. Tang, A 1,8-Naphthyridine-Based Fluorescent Chemodosimeter for the Rapid Detection of Zn^{2+} and Cu^{2+}, *Org. Lett.* 10 (2008) 5115–5118.

[11] M. Rouffet, C. A. F. D. Oliveira, Y. Udi, A. Agrawal, I. Sagi, J. A. McCammon, M. C. Seth, From Sensors to Silencers: Quinoline- and Benzimidazole-Sulfonamides as Inhibitors for Zinc Proteases, *J. Am. Chem. Soc.* 132 (2010) 8232–8233.

[12] T. Budde, Q.A. Minta, J.A. White, A.R. Kay, Imaging Free Zinc in Synaptic Terminals in Live Hippocampal Slices, *Neuroscience* 79 (1997) 347-358.

[13] Z. Dai, G. Proni, D. Mancheno, S. Karimi, N. Berova, J.W. Canary, Detection of Zinc Ions by Differential Circularly Polarized Fluorescence Excitation, *J. Am. Chem. Soc.* 126 (2004) 11760-11761.

[14] F. Qian, C. Zhang, Y. Zhang, W. He, X. Gao, P. Hu, Z. Guo, Visible Light Excitable Zn^{2+} Fluorescent Sensor Derived from an Intramolecular Charge Transfer Fluorophore and Its in Vitro and in Vivo Application, *J. Am. Chem. Soc.* 131 (2009) 1460-1468.

[15] M. Hosseini, Z. Vaezi, M.R. Ganjali, F. Faridbod, S.D. Abkenar, K. Alizadeh, M. Salavati-Niasari, Fluorescence “turn-on” chemosensor for the selective detection of zinc ion based

on Schiff-base derivative, *Spectrochim. Acta, Part A* 75 (2010) 978-982.

[16] X. Wang, C. Qin, E. Wang, Y. Li, N. Hao, C. Hu, L. Xu, Syntheses, Structures, and Photoluminescence of a Novel Class of d^{10} Metal Complexes Constructed from Pyridine-3,4-dicarboxylic Acid with Different Coordination Architectures, *Inorg. Chem.* 43 (2004) 1850-1856.

[17] C. Qin, X. Wang, E. Wang, L. Xu, Layered zinc (II) and cadmium (II) dicarboxylates with aromatic chelate ligand-syntheses, crystal structures and luminescent properties, *J. Mol. Struct.* 738 (2005) 91-98.

[18] L. Wen, Y. Li, D. Dang, Z. Tilan, Z. Ni, Q. Meng, Syntheses, crystal structures and luminescent properties of two new 1D d^{10} coordination polymers constructed from 2,2`-bibenzimidazole and 1,4-benzenedicarboxylate, *J. Solid State Chem.* 178 (2005) 3336-3341.

[19] A. Majumder, G.M. Rosair, A. Mallick, N. Chattopadhyay, S. Mitra, Carboxylatodirhodium(II) complexes with orthometallated tris(p-methoxyphenyl)phosphine and their reactions with pyrazole and imidazole, *Polyhedron* 25 (2006) 1994-2006.

[20] (a) S. Muthu, Z. Ni, J. Vittal, Photoluminescent coordination polymers of d10 metals with 4,40-dipyridylsulfide (dps), *Inorg. Chim. Acta* 358 (2005) 595-605; (b) S.M. Yue, H.B. Xu, J.F. Ma, Z.M. Su, Y.H. Kan, H.J. Zhang, Design and syntheses of blue luminescent zinc(II) and cadmium(II) complexes with bidentate or tridentate pyridyl-imidazole ligands, *Polyhedron* 25 (2006) 635-644.

[21] T. Z. Yu, K. Zhang, Y. Zhao, C. Yang, H. Zhang, D. Fan, W. Dong, A new trinuclear zinc(II) complex possessing five- and six-coordinated central ions and its photoluminescent properties, *Inorg. Chem. Commun*. 10 (2007) 401-403.

[22] W. H. Hsieh, C.-F. Wan, D.-J. Liao, A.-T. Wu, A turn-on Schiff base fluorescence sensor for zinc ion, *Tetrahedron Lett.*, 53 (2012) 5848-5851.

[23] P. Roy, M. Manassero, K. Dhara, P. Banerjee, Synthesis, characterization and fluorescence properties of hexanuclear zinc(II) complexes, *Polyhedron* 28 (2009) 1133-1137.

[24] T. Kawamoto, M. Nishiwaki, Y. Tsunekawa, K. Nozaki, T. Konno, Synthesis and Characterization of Luminescent Zinc(II) and Cadmium(II) Complexes with N,S-Chelating Schiff Base Ligand, *Inorg. Chem.* 47 (2008) 3095-3104.

[25] Z. Zhou, W. Li, X. Hou, L. Chen, X. Hao, C. Redshaw, W. -H. Sun. Synthesis, structure and photophysical properties of 2-benzhydryl-4-methyl-6- (aryliminomethyl)phenol ligands and the zinc complexes thereof, *Inorg. Chim. Acta* 392 (2012) 292-299

[26] J. -J. Xia, Z. Zhou, W. Li, H. -Q. Zhang, C. Redshaw, W. -H. Sun, Synthesis, Structure and Fluorescent Properties of 2-(1H-Benzoimidazol-2-yl) quinolin-8-ols and Their Zinc Complexes, *Inorg. Chim. Acta* 394 (2013) 569-575.

[27] Z. Zhou, W. Li, X. Hao, C. Redshaw, L. -Q. Chen, and W. -H. Sun, 6-Benzhydryl-4-methyl-2-(1H-benzoimidazol-2-yl)phenol ligands and their zinc complexes: Syntheses, characterization and photoluminescence behaviour, *Inorg. Chim. Acta* 392 (2012) 345-353.

[28] L.Salmon, P.Thury, E. Rivire, Ephritikhine, Synthesis, Structure, and Magnetic Behavior of a Series of Trinuclear Schiff Base Complexes of 5f (U^{IV}, Th^{IV}) and 3d (Cu^{II}, Zn^{II}) Ions, *Inorg. Chem.* 45 (2006) 83-93

[29] D.M. Epstein, S. Choudhary, M. R. Churchill, K.M. Keil, A.V. Eliseev, J.R. Morrow, Chloroform-Soluble Schiff-Base Zn(II) or Cd(II) Complexes from a Dynamic Combinatorial Library, *Inorg. Chem.* 40 (2001) 1591-1596

[30] Y. Xu, J. Meng, L. Meng, Y. Dong, Y. Cheng, C. Zhu. A Highly Selective Fluorescence-Based Polymer Sensor Incorporating an (R,R)-Salen Moiety for Zn^{2+} Detection, *Chem. Eur. J.* 16 (2010)

12898-12903

[31] R. Joseph, J. P. Chinta, C. P. Rao, Lower Rim 1,3-Diderivative of Calix[4]arene-Appended Salicylidene Imine (H_2L): Experimental and Computational Studies of the Selective Recognition of H_2L toward Zn^{2+} and Sensing Phosphate and Amino Acid by [ZnL], *J. Org. Chem.* 75 (2010) 3387-3395.

[32] B. Pedras, E. Oliveira, H. Santos, L. Rodriguez, R. Grehuet, T. Avils, J. L. Capel, C. Lodeiro, A new tripodal poly-imine indole-containing ligand: Synthesis, complexation, spectroscopic and theoretical studies, *Inorg. Chim. Acta* 362 (2009) 2627-2635

[33] A. O. Eseola, W. Li, W.-H. Sun, M. Zhang, L. W. Xiao, J. A. O. Woods, Luminescent properties of some imidazole and oxazole based heterocycles: Synthesis, structure and substituent effects, *Dyes and Pigments* 88 (2011) 262-273

[34] A. O. Eseola, W. Li, R. Gao, M. Zhang, X. Hao, T. Liang, N. O. Obi-Egbedi, W.-H. Sun, Syntheses, Structures, and Fluorescent Properties of 2-(1H-Imidazol-2-yl)phenols and Their Neutral Zn(II) Complexes, *Inorg. Chem.* 48 (2009) 9133.

[35] M. Shen, W. Zhang, K. Nomura, W.-H. Sun, Synthesis and characterization of organoaluminum compounds containing quinolin-8-amine derivatives and their catalytic behaviour for ring-opening polymerization of ε-caprolactone, *Dalton Trans.*, **2009**, 9000-9009.

[36] S. K. Dogra, Spectral characteristics of 2-(40-amino-3-pyridyl)benzimidazole: Effects of solvent and acid or base concentration, *J. Lumin.* 118 (2006) 45-60.

[37] S. Banthia, A. Samanta, A New Strategy for Ratiometric Fluorescence Detection of Transition Metal Ions, *J. Phys. Chem. B* 110 (2006) 6437-6440.

[38] (a) L.Wen, Y. Li, Z. Lu, J. Lin, C. Duan, Q. Meng, Syntheses and Structures of Four d^{10} Metal-Organic Frameworks Assembled with Aromatic Polycarboxylate and bix [bix

=1,4-Bis(imidazol-1-ylmethyl)benzene], *Cryst Growth. Des*. 6 (2006) 530-537. (b) L. Wen, Z. Lu, J. Lin, Z. Tian, H. Zhu, Q. Meng, Syntheses, Structures, and Physical Properties of Three Novel Metal−Organic Frameworks Constructed from Aromatic Polycarboxylate Acids and Flexible Imidazole-Based Synthons, *Cryst. Growth. Des.* 7 (2007) 93-99. (c) L.-P. Zhang, J.-F. Ma, J. Yang, Y.-Y. Pang, J.-C. Ma, Series of 2D and 3D Coordination Polymers Based on 1,2,3,4-Benzenetetracarboxylate and *N*-Donor Ligands: Synthesis, Topological Structures, and Photoluminescent Properties, *Inorg. Chem.* 49 (2010) 1535-1550.

[39] D. Das, B.G. Chand, K.K. Sarker, J. Dinda, C. Sinha, Zn(II)-azide complexes of diimine and azoimine functions: Synthesis, spectra and X-ray structures, *Polyhedron* 25 (2006) 2333-2340.

[40] S. Santra, G. Krishnamoorthy, S.K. Dogra, Spectral characteristics of the methylated derivatives of 2-(20-aminophenyl)benzimidazole: effects of solvents, *J. Mol. Struct*. 559 (2011) 25-39.

[41] S. Santra, G. Krishnamoorthy, S.K. Dogra, Excited state intramolecular proton transfer in 2-(2`-benzamidophenyl) benzimidazole: effect of solvent, *Chem. Phys. Lett.* 311(1999) 55-61.

[42] G. M. Sheldrick, SHELXTL-97, Program for the Refinement of Crystal Structures University of Göttingen, Germany, 1997.

Also add the reference:

C. Redshaw, M.R.J.Elsegood, J.W.A. Frese, S. Ashby, Y. Chao and A. Mueller, *Chem. Commun*. 48 (2012) 6627-6629.